



**HAL**  
open science

# Compact Root Architecture 2 Promotes Root Competence for Nodulation through the miR2111 Systemic Effector

Pierre Gautrat, Carole Laffont, Florian Frugier

► **To cite this version:**

Pierre Gautrat, Carole Laffont, Florian Frugier. Compact Root Architecture 2 Promotes Root Competence for Nodulation through the miR2111 Systemic Effector. *Current Biology - CB*, 2020, 30 (7), pp.1339-1345.e3. 10.1016/j.cub.2020.01.084 . hal-02916904

**HAL Id: hal-02916904**

**<https://hal.inrae.fr/hal-02916904>**

Submitted on 22 Aug 2022

**HAL** is a multi-disciplinary open access archive for the deposit and dissemination of scientific research documents, whether they are published or not. The documents may come from teaching and research institutions in France or abroad, or from public or private research centers.

L'archive ouverte pluridisciplinaire **HAL**, est destinée au dépôt et à la diffusion de documents scientifiques de niveau recherche, publiés ou non, émanant des établissements d'enseignement et de recherche français ou étrangers, des laboratoires publics ou privés.



Distributed under a Creative Commons Attribution - NonCommercial 4.0 International License

1 **Compact Root Architecture 2 promotes root competence for nodulation through the**  
2 **miR2111 systemic effector**

3 Pierre Gautrat, Carole Laffont, Florian Frugier\*

4

5 Institute of Plant Sciences – Paris Saclay (IPS2), CNRS, U. Paris-Sud, INRA, U. Paris-  
6 Diderot, U. d'Evry, Université Paris-Saclay, Bâtiment 630, rue de Noetzlin, Plateau du  
7 Moulon, 91190 - Gif-sur-Yvette, France

8

9

10 \* Lead Contact: [florian.frugier@cnrs.fr](mailto:florian.frugier@cnrs.fr)

11

12

13 **Summary**

14 Nitrogen-deprived legume plants form new root organs, the nodules, following a  
15 symbiosis with nitrogen-fixing rhizobial bacteria [1]. As this interaction is beneficial for the  
16 plant but has a high energetic cost, nodulation is tightly controlled by host plants through  
17 systemic pathways (acting at long distance) to promote or limit rhizobial infections and  
18 nodulation depending on earlier infections and on nitrogen availability [2]. In the *Medicago*  
19 *truncatula* model legume, CLE12 (Clavata3/Embryo Surrounding Region 12) and CLE13  
20 signalling peptides produced in nodulated roots act in shoots through the SUNN (Super  
21 Numeric Nodules) receptor to negatively regulate nodulation and therefore autoregulate  
22 nodule number [3–5]. Conversely, CEP (C-Terminally Encoded Peptides) signalling peptides  
23 produced in nitrogen-starved roots act in shoots through the CRA2 (Compact Root  
24 Architecture 2) receptor to promote nodulation already in the absence of rhizobia [6–9]. We  
25 show in this study that a downstream shoot-to-root signalling effector of these systemic  
26 pathways is the shoot-produced miR2111 microRNA [10] that negatively regulates *TML1*  
27 (*Too Much Love 1*) and *TML2* [11] transcripts accumulation in roots, ultimately promoting  
28 nodulation. Low nitrogen conditions and CEP1 signalling peptides induce in the absence of  
29 rhizobia the production of miR2111 depending on CRA2 activity in shoots, thus favoring root  
30 competence for nodulation. Together with the SUNN pathway negatively regulating the same  
31 miR2111 systemic effector when roots are nodulated, this allows a dynamic fine-tuning of the  
32 nodulation capacity of legume roots by nitrogen availability and rhizobial cues.

33

34

35

## 36 **Results and Discussion**

37 Symbiotic nitrogen-fixing nodules form on legume roots when nitrogen is limiting in  
38 soils and when compatible bacteria, collectively referred to as rhizobia, are present in the  
39 rhizosphere (eg *Sinorhizobium medicae* in the case of the *Medicago truncatula* model legume  
40 [12]). These low nitrogen conditions promote the production of CEP signaling peptides in  
41 roots [6] that act systemically in shoots through the CRA2 Leucine-Rich Repeats Receptor-  
42 Like Kinase [7–9]. This would lead to the production of shoot-to-root signaling effectors  
43 ensuring the promotion of the root infection by rhizobia to form symbiotic nitrogen-fixing  
44 nodules. To explore these yet unknown shoot-to-root signaling effectors recruited downstream  
45 of the CEP/CRA2 pathway to promote nodulation under low nitrogen conditions, we analyzed  
46 in *M. truncatula* the symbiotic regulation of two previously identified systemic signals: first,  
47 CEPD proteins acting as shoot-to-root signalling effectors of the *Arabidopsis thaliana* CRA2  
48 orthologous pathway, CEPR1, to promote systemically root nitrogen uptake [13,14]; and  
49 second, the miR2111 microRNA acting in *Lotus japonicus* as a shoot-to-root signalling  
50 effector to promote systemically root nodulation [10], which is negatively regulated by the  
51 HAR1 (Hypernodulation and Aberrant Root 1) pathway [15,16] orthologous to SUNN in *M.*  
52 *truncatula* [3].

53

### 54 **The shoot-produced miR2111 systemic signal, but not MtCEPDs, is downregulated in** 55 **response to rhizobium**

56 CEPD proteins most closely related to *Arabidopsis thaliana* proteins were searched in  
57 the most recent version of the *M. truncatula* genome (v5;  
58 <https://medicago.toulouse.inra.fr/MtrunA17r5.0-ANR/>) [17] to generate a similarity tree  
59 (Figure S1A). Three *M. truncatula* proteins grouped in the same clade as *A. thaliana* CEPD1  
60 and CEPD2 proteins. To determine if these genes could be functional homologs of  
61 *Arabidopsis CEPD* genes and act as systemic effectors, we checked how nitrogen and the  
62 CRA2 pathway regulated their expression, using quantitative RT-PCR (qRT-PCR) in Wild-  
63 Type (WT) and *cra2* plants grown with or without NH<sub>4</sub>NO<sub>3</sub> 5mM (Figure S1B). In shoots, the  
64 expression of two out of the three *MtCEPD* genes, so-called *MtCEPD1* and *MtCEPD2*, was  
65 strongly induced by low nitrogen conditions in WT but not in the *cra2* mutant. This indicates  
66 that *MtCEPD1* and *MtCEPD2* regulation by nitrogen relies on the CRA2 receptor, as reported  
67 for *AtCEPD1* and *AtCEPD2* genes in *Arabidopsis* [14], suggesting that they are *bona fide*

68 functional homologs of *Arabidopsis CEPD* genes. In *M. truncatula* roots, the same  
69 regulations were however observed, indicating that unlike *Arabidopsis*, *CEPD* genes are  
70 expressed in both shoots and roots and regulated by nitrogen. This implies that *MtCEPD*  
71 genes may have local functions to regulate root nitrogen responses. To evaluate a possible  
72 link between these nitrogen-regulated *CEPD* genes and symbiotic nodulation, we then tested  
73 if, similarly as previously observed in response to the high nitrogen treatment, their  
74 expression was also systemically downregulated after a rhizobium inoculation depending on  
75 CRA2. No systemic repression of the expression of these two *MtCEPD* genes was detected in  
76 shoots of plants inoculated by rhizobium (Figure S1C). *MtCEPD* genes were even  
77 upregulated in response to rhizobium in roots, potentially independently of CRA2, thus  
78 showing an antagonistic regulation compared to the high nitrogen treatment. This again  
79 suggests that local regulations and functions of *CEPD* genes likely exist in *M. truncatula*  
80 roots, which may be different however in response to high nitrogen and rhizobium. Overall,  
81 *MtCEPD* genes do not appear as clear-cut candidates to mediate a CRA2-dependent systemic  
82 regulation of nodulation, even though a complex network of nitrogen- and rhizobium-induced  
83 local and systemic regulations may exist.

84 As an alternative, we analyzed if the miR2111, recently proposed in *L. japonicus* as a  
85 shoot-to-root systemic signal downregulated by rhizobium [10], could be a systemic effector  
86 acting downstream of the MtCRA2 pathway. To this aim, we searched for *M. truncatula*  
87 miR2111 precursors in the miRbase (<http://www.mirbase.org>) and MIRMED  
88 (<https://medicago.toulouse.inra.fr/MIRMEDsolexa.cgi>) [18] databases, revealing 18 hits in the  
89 genome, all clustered within a ~75 kb region of the chromosome 7 on the reverse strand  
90 (Figure S1D, Table S1). In order to identify if the miR2111 acts as a systemic effector in  
91 response to rhizobium, we used a split-root experimental system to separate local from  
92 systemic responses. Three conditions were analyzed in parallel: one where one half of the root  
93 system was inoculated or not by rhizobium, defined respectively as “local” versus “systemic”  
94 response compartments; and two homogeneous controls where both halves of the split roots  
95 were either inoculated (“+ Rhizobium”), or not (“- Rhizobium”). Both shoots and roots were  
96 analyzed in parallel (Figure 1A-B). Amongst the 18 miR2111 precursors, none was detected  
97 by qRT-PCR in WT roots, and only six in shoots: the *premiR2111n*, showing the highest  
98 expression level, closely followed by the *premiR2111k* and *premiR2111l*, as well as the  
99 *premiR2111d*, *premiR2111e* and *premiR2111q* having a weaker expression (Figure 1C,  
100 displaying the *premiR2111n* as a representative example; and Figure S1E, showing the similar

101 regulation of all other precursors). The 12 other putative miR2111 precursors could not be  
102 amplified by qRT-PCR despite designing different primer pairs. After rhizobium inoculation,  
103 the expression of the six detectable miR2111 precursors was strongly decreased in shoots and  
104 still not detected in roots (Figure 1C, Figure S1E). A stem-loop qRT-PCR analysis was then  
105 performed to monitor the mature miR2111 accumulation, which accordingly revealed a  
106 decreased accumulation after rhizobium inoculation, not only in shoots but also in each root  
107 compartment (local and systemic ; Figure 1C). This result is in agreement with *L. japonicus*  
108 data and a model where mature miRNAs move systemically from shoots to roots [10],  
109 positioning the miR2111 as an ideal candidate to act as a downstream shoot-to-root systemic  
110 effector of the CRA2 pathway.

111

### 112 **The miR2111 regulates *MtTML* transcripts level in roots and its accumulation is** 113 **repressed in response to rhizobium through the SUNN systemic pathway**

114 In *M. truncatula*, two orthologous *LjTML* genes, *TML1* and *TML2*, encode F-box  
115 proteins previously shown to act in roots to negatively regulate nodule number [11,19,20]. To  
116 determine if the miR2111 post-transcriptional regulation of *TML* transcripts accumulation in  
117 roots is conserved between *L. japonicus* and *M. truncatula* [10], we used two independent  
118 already available “degradome” genome-wide datasets [21,22]. Interestingly, both *MtTML*  
119 transcripts were shown to be cleaved by the miR2111 ([18], Figure S2). To independently  
120 validate the regulation of *MtTML* transcripts by the miR2111, the *premiR2111n* precursor was  
121 overexpressed (p35S:*premiR2111n*, Figure 2C), leading to the accumulation of miR2111  
122 (Figure 2D) and to a reduction of *MtTML* transcripts accumulation (Figure 2E). Conversely,  
123 expression of a mimicry construct inhibiting the action of the miRNA (pUBI:*MIMmiR2111*,  
124 Figure S2C) showed a reduced accumulation of miR2111 (Figure S2D) and an increased  
125 accumulation of *MtTML* transcripts (Figure S2E). Overall, this indicates the functionality of  
126 the miR2111, as well as of the *premiR2111n* precursor, to negatively regulate *TML1* and  
127 *TML2* transcripts accumulation. These two independent experiments additionally revealed a  
128 positive role of the miR2111 on nodule number (Figure 2A-B, Figure S2B and G).

129 We then tested if *TML1* and *TML2* transcripts accumulation was affected by a  
130 rhizobium inoculation using the dedicated split-root experimental system described previously  
131 (Figure 1A-B). Interestingly, these two validated miR2111 target genes were only detected in

132 roots, and their transcripts accumulated in response to rhizobium either locally or systemically  
133 (Figure 1C).

134 As the miR2111/*MtTML* module was previously associated to the Autoregulation Of  
135 Nodulation (AON) pathway in *L. japonicus* [10], we evaluated the conservation of this  
136 systemic regulation in *M. truncatula*. To this aim, we analyzed the expression of the  
137 miR2111/*MtTML* module in the *sun*n mutant (Figure 3A). The repression of the mature  
138 miR2111 accumulation and of miR2111 precursors expression in response to rhizobium was  
139 abolished in the *sun*n mutant compared to WT plants (Figure 3A; Figure S3A). Accordingly,  
140 the level of *TML1/TML2* target transcripts was decreased (Figure 3A). These results  
141 established that the regulation by rhizobium of the miR2111/*MtTML* module relies on the  
142 SUNN AON pathway in *M. truncatula*.

143 Compared to data available in *L. japonicus* [10], an additional functional validation  
144 was provided to sustain the link between the SUNN/HAR1 pathway and the miR2111/*MtTML*  
145 module. The pUBI:*MIMmiR2111* construct inhibiting miR2111 action was expressed in *M.*  
146 *truncatula sun*n mutant roots. The *MIMmiR2111* transgene level correlated with its inhibitory  
147 effect on miR2111 accumulation and with an increased *MtTML* transcripts level (Figure S2C-  
148 E). This miR2111 inhibition was sufficient to rescue the *sun*n mutant supernodulation  
149 phenotype, partially when considering nodule density and to a WT level when considering  
150 nodule number (Figure 2A, Figure S2B and F).

151 Overall, these results indicate that the HAR1/SUNN-dependent downregulation of  
152 miR2111 expression in shoots challenged with rhizobium is conserved between *L. japonicus*  
153 and *M. truncatula*, and that impairing miR2111 action is sufficient to rescue the *sun*n  
154 supernodulation phenotype.

155

156 **The CRA2 receptor activity in shoots is required to maintain a high level of miR2111**  
157 **expression in rhizobial non-inoculated plants, promoting root competence to nodulate**

158 Having validated the miR2111 as a systemic shoot-to-root effector regulating nodule  
159 number, we tested if its accumulation could be promoted by the CRA2 systemic pathway  
160 positively regulating nodulation [9]. Strikingly, expression of all miR2111 precursors  
161 detectable in shoots, and accumulation of the miR2111 in shoots and roots, were strongly  
162 reduced in the *cra2* mutant already before rhizobium inoculation (Figure 3B, Figure S3B).

163 Accordingly, a higher accumulation of *TML1* target transcripts was detected in *cra2* mutant  
164 roots compared to WT plants, even though *TML2* was not deregulated in these experimental  
165 conditions (Figure 3B). In response to rhizobium, the low expression and accumulation of the  
166 miR2111 was maintained in the *cra2* mutant, and strikingly, miR2111 accumulation in WT  
167 rhizobium-inoculated roots was similar to *cra2* non-inoculated roots. This suggests that the  
168 *cra2* mutant inability to nodulate [7,9] may be linked to a basal downregulation of the  
169 miR2111 accumulation. In addition, these results demonstrate that the CRA2 systemic  
170 pathway is critical to positively regulate miR2111 accumulation in rhizobial non-inoculated  
171 plants.

172 These observations prompted us to test if an ectopic expression of the miR2111 was  
173 sufficient to rescue the *cra2* low nodulation phenotype. We therefore transformed *cra2* mutant  
174 roots with the previously described p35S:*premiR2111n* construct. Overexpression of the  
175 *premiR2111n* correlated with an increased miR2111 accumulation and with a decreased  
176 *MtTML* transcripts accumulation (Figure 2C-E). This miR2111 ectopic expression was indeed  
177 sufficient to rescue the low *cra2* mutant nodulation phenotype, even at a WT level when the  
178 *cra2* compact root phenotype was considered by quantifying the nodule density (Figure 2B  
179 and F; Figure S2G).

180 As previous grafting studies showed that the CRA2 pathway promotes nodulation  
181 from shoots [7,9], we then tested if the regulation of the miR2111/*MtTML* module relied on  
182 the activity of CRA2 in shoots and/or in roots. Grafts generated between non-inoculated *cra2*  
183 and WT plants revealed that the CRA2 activity in shoots, but not in roots, was required to  
184 positively regulate *premiR2111n* expression in shoots, as well as miR2111 accumulation in  
185 both shoots and roots (Figure 4A). These results are therefore in agreement with previous  
186 *cra2* mutant grafting nodulation phenotypes [7,9]. Interestingly, under these experimental  
187 conditions, the accumulation of both *MtTML* transcripts was induced in *cra2* mutant  
188 homografted plants. In addition, heterologous grafts revealed that the regulation of *MtTML*  
189 transcripts accumulation also relied on the activity of CRA2 in shoots.

190 Collectively, these results show that the CRA2 pathway positively regulates from  
191 shoots miR2111 expression and accumulation. Noteworthy, increasing the accumulation of  
192 the miR2111 in the *cra2* mutant was sufficient to rescue its low nodulation phenotype.  
193 Overall, this demonstrates that the miR2111/*MtTML* module is a downstream systemic  
194 effector of the CRA2 pathway.

195

196 **Low nitrogen and CEP1 signalling peptides promote systemically miR2111 expression**  
197 **depending on the CRA2 receptor**

198 Low nitrogen availability induces in roots the expression of *CEP* peptide encoding  
199 genes such as *CEP1* [6], which act through the CRA2 systemic pathway to stimulate  
200 nodulation [8,9]. To determine if the miR2111 systemic effector was induced by low nitrogen  
201 availability depending on CRA2, we assessed the transcriptional regulation of the  
202 miR2111/*MtTML* module in WT and *cra2* mutant plants grown on nitrogen depleted or  
203 sufficient conditions (+/- NH<sub>4</sub>NO<sub>3</sub> 5 mM; Figure 4B, Figure S4A). The expression of  
204 miR2111 precursors and the accumulation of miR2111 were higher in the depleted nitrogen  
205 condition compared to the high nitrogen condition, and conversely transcripts accumulation of  
206 both *MtTML* genes was decreased, as expected. In the *cra2* mutant, accumulation of  
207 *premiR2111*, miR2111, and *MtTML* transcripts were similar to WT plants grown on high  
208 nitrogen, correlating again with the mutant inability to nodulate. These results highlight that  
209 the accumulation of the miR2111 systemic effector is promoted by low nitrogen and repressed  
210 not only by rhizobium inoculation but also by high nitrogen. In addition, the higher  
211 accumulation of miR2111 in nitrogen starved plants relies on CRA2.

212 Finally, the role of CEP1 peptides on the regulation of the miR2111 systemic effector  
213 was evaluated using an ectopic expression strategy (*p35S:CEP1* [6]) in WT and *cra2* mutant  
214 plants (Figure 4C, Figure S4B). *CEP1* transgene overexpression (Figure S4B) promoted the  
215 expression of *premiR2111* precursors and miR2111 accumulation, whereas transcripts  
216 accumulation of both *MtTML* genes was decreased. In *cra2* mutants, *CEP1* overexpression  
217 did not affect the miR2111/*MtTML* module. These results indicate that CEP1 promotes  
218 miR2111 accumulation depending on the CRA2 pathway.

219 Altogether, we showed that under low nitrogen conditions, CEP1 signalling peptides  
220 act through the CRA2 receptor to promote in shoots the expression of miR2111 precursors,  
221 and consequently the accumulation of miR2111 in both shoots and roots, leading to the  
222 repression of *MtTML* target transcripts accumulation in roots (Graphical Abstract). As the  
223 miR2111 promotes nodulation and can rescue the *cra2* low nodulation phenotype, this  
224 suggests that, under low nitrogen conditions, the CRA2 pathway actively maintains the root  
225 competency for nodulation through the downstream miR2111 systemic effector. Together  
226 with results obtained in *L. japonicus* [10], our data additionally revealed that the miR2111

227 systemic effector is at the crossroad of two systemic pathways involving different families of  
228 signalling peptides, CLE and CEP, which are regulating antagonistically nodulation  
229 depending on nitrogen availability and rhizobial cues. The coordination of these two systemic  
230 regulatory pathways ultimately ensures a dynamic adaptation of nodule number homeostasis  
231 in nutrient heterogeneous and fluctuating environments (Graphical Abstract). Finally, it  
232 remains open that *MtCEPD* genes, beside regulating different aspects of root system  
233 architecture and nitrate uptake depending on *CRA2*, as anticipated from the *cra2* “compact  
234 root architecture” mutant phenotype and as proposed in Arabidopsis [13], may also  
235 participate in regulating nodulation. If so, *MtCEPD* transcriptional regulations suggest that a  
236 combination of local and systemic functions induced in response to nitrogen and/or rhizobium  
237 may exist.

238

### 239 **Acknowledgements**

240 We thank at IPS2 Christine Lelandais-Brière for help in using the MIRMED database  
241 and fruitful discussions, Hélène Proust for suggestions with small RNA protocols, Corentin  
242 Moreau for some primer design, and Ambre Miassod for cheerful help on some experiments  
243 and for the graphical abstract drawing. We also thank Pascal Gamas (LIPM, Castanet-  
244 Tolosan, France) for sharing preliminary unpublished genomic and transcriptomic analyses  
245 that helped the exhaustive identification of premiR2111 loci in the *M. truncatula* genome; and  
246 Marc Lepetit (LRSV, Montpellier, France) for suggestions on low/high nitrogen conditions to  
247 be used. Golden Gate binary vectors were provided by the Engineering Nitrogen Symbiosis  
248 for Africa (ENSA) initiative (<https://www.ensa.ac.uk/>). P.G. was the recipient of a fellowship  
249 from the Paris-Sud/Paris-Saclay University. The work was supported by the Agence  
250 Nationale de la Recherche (ANR) “PSYCHE” project (ANR-16-CE20-0009-01).

251

### 252 **Authors contributions**

253 P.G. performed most of the experiments, with help from C.L. F.F. conceived the project. P.G.  
254 and F.F. wrote the manuscript.

255

### 256 **Declaration of Interests**

257 The authors declare no competing interest.

258

259 **Figure legends**

260 **Figure 1. Systemic accumulation of the miR2111 microRNA and of *MtTML* target**  
261 **transcripts is anti-correlated in response to rhizobium**

262 (A) Image of a *M. truncatula* plant growing in an *in vitro* split-root experimental system  
263 (scale bar = 1cm). (B) Split-root experimental design with plants either inoculated with  
264 rhizobium (“+ Rhizobium” in orange), or not (“- Rhizobium” in blue), or inoculated on only  
265 one half of the root system (“Split” plants, the inoculated side being called “Local” and the  
266 non-inoculated side “Systemic”). (C) Transcript levels of *premiR2111n*, *TML1* and *TML2*  
267 genes were analyzed by qRT-PCR and the accumulation of the major miR2111 isoform by  
268 stem-loop qRT-PCR, in shoots and roots of Wild-Type (WT) plants grown in the split-root  
269 experimental system described in (B), five days post inoculation (5dpi). Data were normalized  
270 to 1 relatively to the non-inoculated control, as indicated with dotted lines. A pool of seven  
271 biological replicates (n>35 plants per condition) is shown, and error bars represent standard  
272 deviations. A Student t-test was performed to assess statistical differences with the non-  
273 inoculated control (\*P<0.05; \*\*P<0.001; \*\*\*P<0.0001). ND stands for Not Detected. See also  
274 Table S1 and Figure S1.

275 **Figure 2. Modulation of miR2111 accumulation affects *MtTML* transcripts level and**  
276 **rescues the *sunn* and *cra2* mutant nodulation phenotypes**

277 (A) Nodule density (nodules/mg of root dry weight) of Wild-Type (WT) and *sunn* mutant  
278 roots transformed with a pUBI:GUS control vector or a pUBI:MIMmiR2111 construct, 14  
279 days post rhizobium inoculation (14dpi). One representative biological experiment out of  
280 three is shown, and a Kruskal-Wallis statistical test was performed to assess significant  
281 differences shown by letters ( $\alpha$ <0.05; n>25 plants per condition). (B) Nodule density  
282 (nodules/mg of root dry weight) of Wild-Type (WT) and *cra2* mutant roots transformed with  
283 an empty vector or a p35S:*premiR2111n* construct, 14dpi. One representative biological  
284 experiment out of three is shown, and a Kruskal-Wallis statistical test was performed to assess  
285 significant differences shown by letters ( $\alpha$ <0.05; n>20 plants per condition). (C-E) The  
286 transcript level of the *premiR2111n* (C), the accumulation of the miR2111 (D), and of *TML1*  
287 and *TML2* transcripts (E) were analyzed by qRT-PCR in representative roots from three  
288 biological replicates (n=6 plants per condition) grown as described in (B), 5dpi. Data were  
289 normalized to 1 for each genotype relatively to empty vector control roots, as indicated with  
290 dotted lines, to highlight the effect of the miR2111 overexpression, and error bars represent

291 standard deviations. A Student t-test was performed to assess statistical differences with the  
292 empty vector controls (\*P<0.05; \*\*P<0.001; \*\*\*P<0.0001). (F) Details of representative  
293 roots analyzed in (B). White arrows indicate nodules (scale bars = 1cm). See also Figure S2.

294 **Figure 3. miR2111 accumulation is negatively regulated by the SUNN pathway in**  
295 **response to rhizobium and positively by the CRA2 pathway in the absence of rhizobium**

296 (A) Transcript levels of *premiR2111n*, *TML1* and *TML2* genes were analyzed by qRT-PCR  
297 and the accumulation of the major miR2111 isoform by stem-loop qRT-PCR, in shoots and  
298 roots of Wild-Type (WT) and *sun* mutant plants grown in the split-root experimental system  
299 described in Figure 1B, five days post rhizobium inoculation (5dpi). Data were normalized to  
300 1 relatively to the non-inoculated WT control, as indicated with dotted lines. A pool of three  
301 biological replicates (n>13 plants per conditions) is shown and error bars represent standard  
302 deviations. A Student t-test was performed to assess statistical differences with the non-  
303 inoculated WT control (\*P<0.05; \*\*P<0.001; \*\*\*P<0.0001). (B) Transcript levels of  
304 *premiR2111n*, *TML1* and *TML2* genes were analyzed by qRT-PCR and the accumulation of  
305 the miR2111 by stem-loop qRT-PCR, in shoots and roots of WT and *cra2* mutant plants  
306 grown in the split-root experimental system described in Figure 1B, 5dpi. Data were  
307 normalized to 1 relatively to the non-inoculated WT control, as indicated with dotted lines. A  
308 pool of three biological replicates (n>16 plants per condition) is shown and error bars  
309 represent standard deviations between biological replicates. A Student t-test was performed to  
310 assess statistical differences with the non-inoculated WT control (\*P<0.05; \*\*P<0.001;  
311 \*\*\*P<0.0001). See also Figure S3.

312 **Figure 4. Low nitrogen and CEP1 peptides promote miR2111 accumulation depending**  
313 **on the CRA2 receptor**

314 (A) Transcript levels of *premiR2111n*, *TML1* and *TML2* genes were analyzed by qRT-PCR  
315 and the accumulation of the major miR2111 isoform by stem-loop qRT-PCR, in shoots and  
316 roots of grafted Wild-Type (WT) and *cra2* mutant plants seven days after transfer on a  
317 nitrogen deprived medium. Data were normalized to 1 relatively to the WT homografted  
318 control, as indicated with dotted lines. A pool of three biological replicates (n>16 plants per  
319 condition) is shown and error bars represent standard deviations between biological replicates.  
320 A Student t-test was performed to assess statistical differences with the WT homografted  
321 control (\*P<0.05; \*\*P<0.001; \*\*\*P<0.0001). (B) Transcripts level of *premiR2111n*, *TML1*  
322 and *TML2* were analyzed by qRT-PCR and accumulation of miR2111 by stem-loop qRT-

323 PCR, in shoots and roots of WT and *cra2* mutant plants 12 days after transfer on a nitrogen  
324 deprived medium (- N) or with nitrogen (+ NH<sub>4</sub>NO<sub>3</sub> 5mM). Data were normalized relatively  
325 to the nitrogen deprived WT control, as indicated with dotted lines. A pool of two biological  
326 replicates (n>9 plants per condition) is shown, and error bars represent standard deviations. A  
327 Student t-test was performed to assess statistical differences with the nitrogen deprived WT  
328 control (\*P<0.05; \*\*P<0.001; \*\*\*P<0.0001). ND stands for Not Detected. (C) Transcripts  
329 level of *premiR2111n*, *TML1* and *TML2* were analyzed by qRT-PCR and accumulation of  
330 miR2111 by stem-loop qRT-PCR, in shoots and roots of WT and *cra2* mutant plants  
331 transformed with an Empty Vector (EV) or a p35S:*CEP1* construct 12 days after transfer on a  
332 NH<sub>4</sub>NO<sub>3</sub> 5mM medium. Data were normalized relatively to the WT EV control, as indicated  
333 with dotted lines. One biological replicate out of two is shown (n>5 per condition and  
334 replicate), and error bars represent standard deviations. A Student t-test was performed to  
335 assess statistical differences with the WT EV control (\*P<0.05; \*\*P<0.001; \*\*\*P<0.0001).  
336 ND stands for Not Detected. See also Figure S4.

337

338

339

340

341

342

343

344

345

346

347

348

349

350 **STAR METHODS**

351 **LEAD CONTACT AND MATERIALS AVAILABILITY**

352 Further information and requests for resources and reagents should be directed to and  
353 will be fulfilled by the Lead Contact, Florian Frugier (florian.frugier@cnr.fr).

354 All unique/stable reagents generated in this study (p35S:*premiR2111n*, pUBI:*GUS* and  
355 pUBI:*MIMmiR2111* constructs) are available from the Lead Contact with a completed  
356 Materials Transfer Agreement.

357

358 **EXPERIMENTAL MODEL AND SUBJECT DETAILS**

359 The *Medicago truncatula* Jemalong A17 wild-type genotype, as well as the *cra2-11*  
360 mutant that contains an insertion in the region encoding the kinase domain (Key Resources  
361 Table), and the *sunm-4* mutant that has a mutation introducing a stop codon at the residue 58  
362 (Key Resources Table), were used in this study. Seeds were scarified for 3 minutes using  
363 pure sulfuric acid (Sigma), washed four times with water and sterilized for 20 minutes with  
364 Bayrochlore (3.75g/L, Bayrol, Chlorofix). Seeds were then washed again, transferred onto a  
365 water/BactoAgar plate (Sigma), stratified for four days in the dark at 4°C, and then  
366 germinated at 24°C in the dark for one night.

367 For *in vitro* split-root and grafting experiments, seedlings were placed onto a growth  
368 culture paper (Mega International, <https://mega-international.com/>) in vertical 1,5%  
369 BactoAgar plates containing Fahraeus medium [28] (0.132 g/L CaCl<sub>2</sub>, 0.12 g/L MgSO<sub>4</sub>.7H<sub>2</sub>O,  
370 0.1 g/L KH<sub>2</sub>PO<sub>4</sub>, 0.075 g/L Na<sub>2</sub>HPO<sub>4</sub>.2H<sub>2</sub>O, 5 mg/L Fe-citrate, and 0.07 mg/L each of  
371 MnCl<sub>2</sub>.4H<sub>2</sub>O, CuSO<sub>4</sub>.5H<sub>2</sub>O, ZnCl<sub>2</sub>, H<sub>3</sub>BO<sub>3</sub>, and Na<sub>2</sub>MoO<sub>4</sub>.2H<sub>2</sub>O) with nitrogen (1mM  
372 NH<sub>4</sub>NO<sub>3</sub>, F+), in a growth chamber with a 16h photoperiod, a light intensity of 150μE, and a  
373 temperature of 24°C. For split-root experiments, roots were then cut five days post-  
374 germination (dpg), seedlings were grown in between two growth papers for one week, and an  
375 additional week without growth paper. Plants with two equivalent roots were then selected  
376 and transferred onto Fahraeus medium without nitrogen (F-) on a plate where the agar was  
377 separated in two halves. For grafting experiments, roots were cut from shoots also at five dpg  
378 and grafts were generated by cutting plants hypocotyls and reassembling roots and shoots of  
379 appropriate genotypes together within a capillary tube, as described in [9] and in the *M.*

380 *truncatula* handbook (chapter Cuttings and Grafts;  
381 <http://www.noble.org/medicagohandbook/>). After two weeks, grafted plants were transferred  
382 onto F- medium plates.

383 For composite plants experiments (see Method Details), plants were transferred *in*  
384 *vitro* on an F medium with or without  $\text{NH}_4\text{NO}_3$  5mM, for high/low nitrogen experiments; and  
385 on an F medium with  $\text{NH}_4\text{NO}_3$  5mM for the CEP1 overexpression experiment. For composite  
386 plant nodulation experiments, plants were transferred into a pot containing a sand:perlite 1:3  
387 mixture and placed in a growth chamber with a 16h photoperiod, a light intensity of  $150\mu\text{E}$ , a  
388 temperature of  $24^\circ\text{C}$ , and 65% of relative humidity. Plants were watered with an “i” growth  
389 medium with low nitrogen ( $\text{KNO}_3$  0.25mM) [29]. Stock solution of this medium is obtained  
390 by mixing 250mL of each of the following components:  $\text{KNO}_3$  20,2g/L,  $\text{KH}_2\text{PO}_4$  27,2g/L,  
391  $\text{CaCl}_2$  ( $2\text{H}_2\text{O}$ ) 73g/L,  $\text{MgSO}_4$  ( $7\text{H}_2\text{O}$ ) 24,6g/L,  $\text{K}_2\text{SO}_4$  43,5g/L,  $\text{EDTA}_2\text{Na}_2\text{Fe}$  8,2g/L. 13,5mL  
392 of the following mix is then added:  $\text{H}_3\text{BO}_3$  11g/L,  $\text{MnSO}_4$  6,2g/L,  $\text{KCl}$  10g/L,  $\text{ZnSO}_4$  ( $7\text{H}_2\text{O}$ )  
393 1g/L,  $(\text{NH}_4)_6\text{Mo}_7\text{O}_{24}$  ( $4\text{H}_2\text{O}$ ) 1g/L,  $\text{CuSO}_4$  ( $5\text{H}_2\text{O}$ ) 0.5g/L,  $\text{H}_2\text{SO}_4$  95% 0.5mL. This stock  
394 solution is diluted 40 times with deionized water before use

395 Two different strains of rhizobium were used in this study: *Sinorhizobium meliloti*  
396 1021 (Key Ressources Table) for early stage nodulation *in vitro* experiments, and  
397 *Sinorhizobium medicae* WSM419 (Key Ressources Table) for late stage nodulation  
398 experiments in pots. Both strains were grown for 24 hours at  $30^\circ\text{C}$  in a Yeast Broth Extract  
399 medium (YEB), supplemented with  $100\mu\text{g/ml}$  streptomycin (Sigma) or  $50\mu\text{g/mL}$   
400 chloramphenicol (Sigma) for the Sm1021 or the WSM419 strain, respectively. Rhizobium  
401 inoculations were performed using an overnight grown bacterial culture diluted at an  $\text{OD}_{600\text{nm}}$   
402 = 0.05 for pots and at an  $\text{OD}_{600\text{nm}}$  = 0.2 for *in vitro* split-root experiments. Composite and  
403 split-root plants were inoculated with rhizobium seven days after transfer to pots and to F-  
404 plates, respectively. Nodule number and root dry weight were measured at 14 days post  
405 rhizobium inoculation (dpi).

406

## 407 **METHOD DETAILS**

### 408 Cloning procedures and root transformation

409 The pUBI:*MIMmiR2111* (Key Ressources Table) construct was generated using  
410 Golden Gate cloning [30] and a synthetic *MIMmiR2111* gene (Twist Bioscience,

411 <http://www.twistbioscience.com/>; sequence indicated in the Table S2) as described in [31] in  
412 the EC50507 binary vector (<https://www.ensa.ac.uk/>). A pUBI:GUS control vector was also  
413 generated using the same strategy in the same binary vector.

414 The p35S:*premiR2111n* (Key Ressources Table) construct was obtained by restriction  
415 cloning using the binary vector pMF2 (Key Ressources Table). The *premiR2111n* gene was  
416 amplified from *M. truncatula* A17 genomic DNA by Polymerase Chain Reaction (PCR) using  
417 forward and reverse primers flanked by BamHI and EcoRI restriction sites, respectively (the  
418 list of primers used is given in the Table S2). The *premiR2111n* PCR amplicon was then  
419 integrated into the pMF2 vector downstream of a 35S:CaMV (Cauliflower Mosaic Virus)  
420 cassette using these restriction sites. The p35S:*CEP1* construct was generated in [6] (Key  
421 Ressources Table).

422 Clonings were generated using thermocompetent DH5 $\alpha$  *Escherichia coli* (Key  
423 Ressources Table), and final binary vectors used for plant transgenesis were transformed into  
424 *Agrobacterium rhizogenes* Arqua1 (Key Ressources Table).

425 “Composite plants” were obtained *in vitro* by cutting germinated seedling roots and  
426 dipping the root sections into a bacterial mat of the *A. rhizogenes* Arqua1 strain containing the  
427 construct of interest, as described in [24], followed by two weeks of kanamycin selection  
428 (25 $\mu$ g/mL) on a F+ medium.

#### 429 Long and small RNA extraction and qRT-PCR

430 Total RNAs were extracted using the miRvana kit (Key Ressources Table) or the  
431 Quick-RNA Miniprep kit (Key Ressources Table), from non-inoculated or five dpi plants for  
432 split-roots, from non-inoculated plants for the MIMmiR2111, from 12 days after transfer  
433 (corresponding to five dpi) for miR2111 overexpression experiments, from seven days after  
434 transfer on the F- medium for grafts, and from 12 days after transfer for nitrogen response and  
435 CEP1 overexpression experiments. RNAs were then treated with a DNase1 RNase-free  
436 (Thermofisher) following manufacturer instructions. cDNAs were obtained using the  
437 SuperScript III Reverse Transcriptase (200U/ $\mu$ L, Key Ressources Table) following  
438 manufacturer instructions. A stem-loop Reverse Transcription (RT) was performed to amplify  
439 each specific mature miRNA by including amplification adapters (listed in the Table S2) to  
440 the RT mix, as described in [31]. Two independent cDNA samples were generated from each  
441 RNA sample as technical replicates.

442 Gene expression was analyzed by quantitative RT-PCR (qRT-PCR) on a  
443 LightCycler480 apparatus (Roche) using the Light Cycler 480 SYBR Green I Master mix  
444 (Key Ressources Table) and dedicated specific primers to amplify genes of interest (listed in  
445 the Table S2). Forty amplification cycles (15s at 95°C, 15s at 60°C, 15s at 72°C) were  
446 performed, as well as a final fusion curve from 60 to 95°C to assess primers specificity.  
447 Amplicons were independently sequenced to confirm their specificity. Primer efficiency was  
448 systematically tested and only primers with efficiency over 90% were retained. Gene  
449 expression was normalized using two different reference genes, *MtActin11* and *MtRNA*  
450 *Binding Protein 1 (MtRBPI)*, while miRNA accumulation was normalized using the miR162  
451 mature miRNA and the U6 small nuclear RNA [32]. In figures, *MtActin11* and miR162  
452 references were selected to normalize the data.

### 453 Similarity tree building

454 The similarity tree was built using the Seaview4 software (Key Ressources Table).  
455 Proteins were aligned with MUSCLE, alignments were optimized with Gblocks, and the tree  
456 was generated based on the bootstrap method (1000 replicates).

457

## 458 **QUANTIFICATION AND STATISTICAL ANALYSIS**

459 Statistical analyses were performed with the XLSTAT software (Key Ressources  
460 Table) using Kruskal-Wallis tests for phenotyping experiments and Student t-tests for qRT-  
461 PCR experiments. Results of statistical tests are represented by letters or stars in Figures.  
462 Specificities of each test and of graphical representations are mentioned in each Figure legend  
463 and below: n represents the number of plants analyzed; for qRT-PCR data, means and  
464 standard deviations (SD) are shown, and for plant phenotyping, medians and quartiles are  
465 shown. Statistical significance was defined as follows:  $\alpha < 0.05$  for Kruskal-Wallis tests; and \*,  
466  $P < 0.05$ , \*\*,  $P < 0.001$ , and \*\*\*,  $P < 0.0001$  for Student t-tests. No data were excluded in this  
467 study.

468

## 469 **DATA AND CODE AVAILABILITY**

470 The datasets supporting the current study have not been deposited in any public  
471 repository but are available from the Lead Contact upon request.

472 **References**

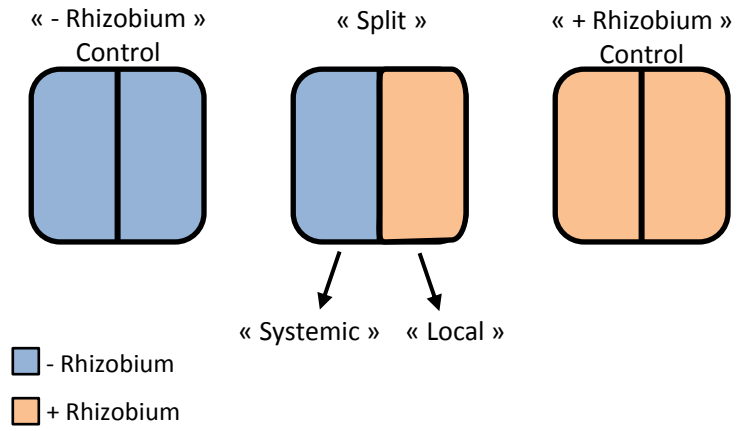
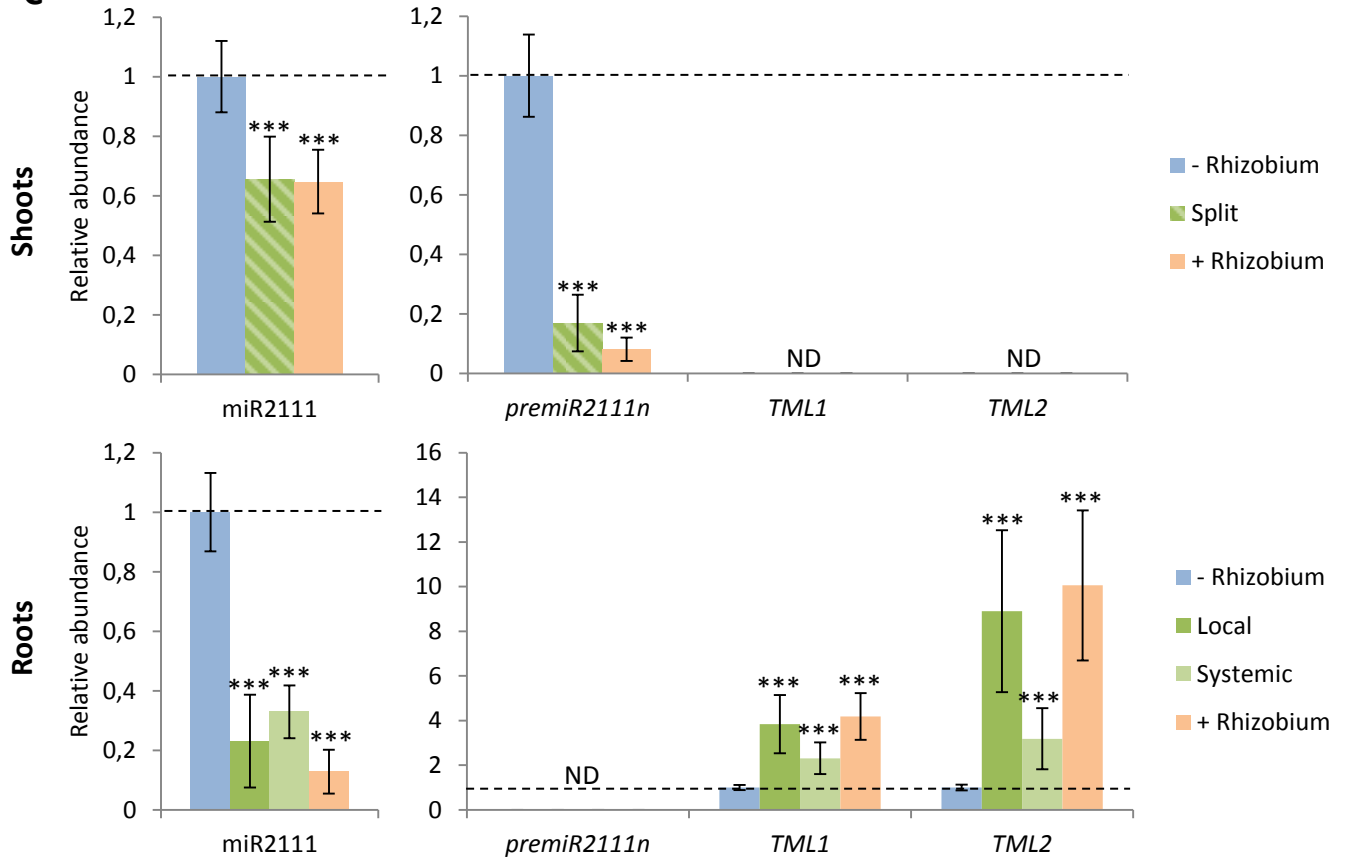
- 473 1. Suzuki, T., Yoro, E., and Kawaguchi, M. (2015). Leguminous Plants: Inventors of Root  
474 Nodules to Accommodate Symbiotic Bacteria. *International Review of Cell and*  
475 *Molecular Biology*. *316*, 111-158.
- 476 2. Okamoto, S., Tabata, R., and Matsubayashi, Y. (2016). Long-distance peptide signaling  
477 essential for nutrient homeostasis in plants. *Curr. Opin. Plant Biol.* *34*, 35–40.
- 478 3. Schnabel, E., Journet, E.P., De Carvalho-Niebel, F., Duc, G., and Frugoli, J. (2005).  
479 The *Medicago truncatula* SUNN gene encodes a CLV1-like leucine-rich repeat  
480 receptor kinase that regulates nodule number and root length. *Plant Mol. Biol.* *58*, 809–  
481 822.
- 482 4. Mortier, V., den Herder, G., Whitford, R., van de Velde, W., Rombauts, S.,  
483 D’haeseleer, K., Holsters, M., and Goormachtig, S. (2010). CLE peptides control  
484 *Medicago truncatula* nodulation locally and systemically. *Plant Physiol.* *153*, 222–237.
- 485 5. Mortier, V., De Wever, E., Vuylsteke, M., Holsters, M., and Goormachtig, S. (2012).  
486 Nodule numbers are governed by interaction between CLE peptides and cytokinin  
487 signaling. *Plant J.* *70*, 367–376.
- 488 6. Imin, N., Mohd-Radzman, N.A., Ogilvie, H.A., and Djordjevic, M.A. (2013). The  
489 peptide-encoding CEP1 gene modulates lateral root and nodule numbers in *Medicago*  
490 *truncatula*. *J. Exp. Bot.* *64*, 5395–5409.
- 491 7. Huault, E., Laffont, C., Wen, J., Mysore, K.S., Ratet, P., Duc, G., and Frugier, F.  
492 (2014). Local and Systemic Regulation of Plant Root System Architecture and  
493 Symbiotic Nodulation by a Receptor-Like Kinase. *PLoS Genet.* *10*, e1004891.
- 494 8. Mohd-Radzman, N.A., Laffont, C., Ivanovici, A., Patel, N., Reid, D., Stougaard, J.,  
495 Frugier, F., Imin, N., and Djordjevic, M.A. (2016). Different pathways act downstream  
496 of the CEP peptide receptor CRA2 to regulate lateral root and nodule development.  
497 *Plant Physiol.* *171*, 2536–2548.
- 498 9. Laffont, C., Huault, E., Gautrat, P., Endre, G., Kalo, P., Bourion, V., Duc, G., and  
499 Frugier, F. (2019). Independent Regulation of Symbiotic Nodulation by the SUNN  
500 Negative and CRA2 Positive Systemic Pathways. *Plant Physiol.* *180*, 559–570.

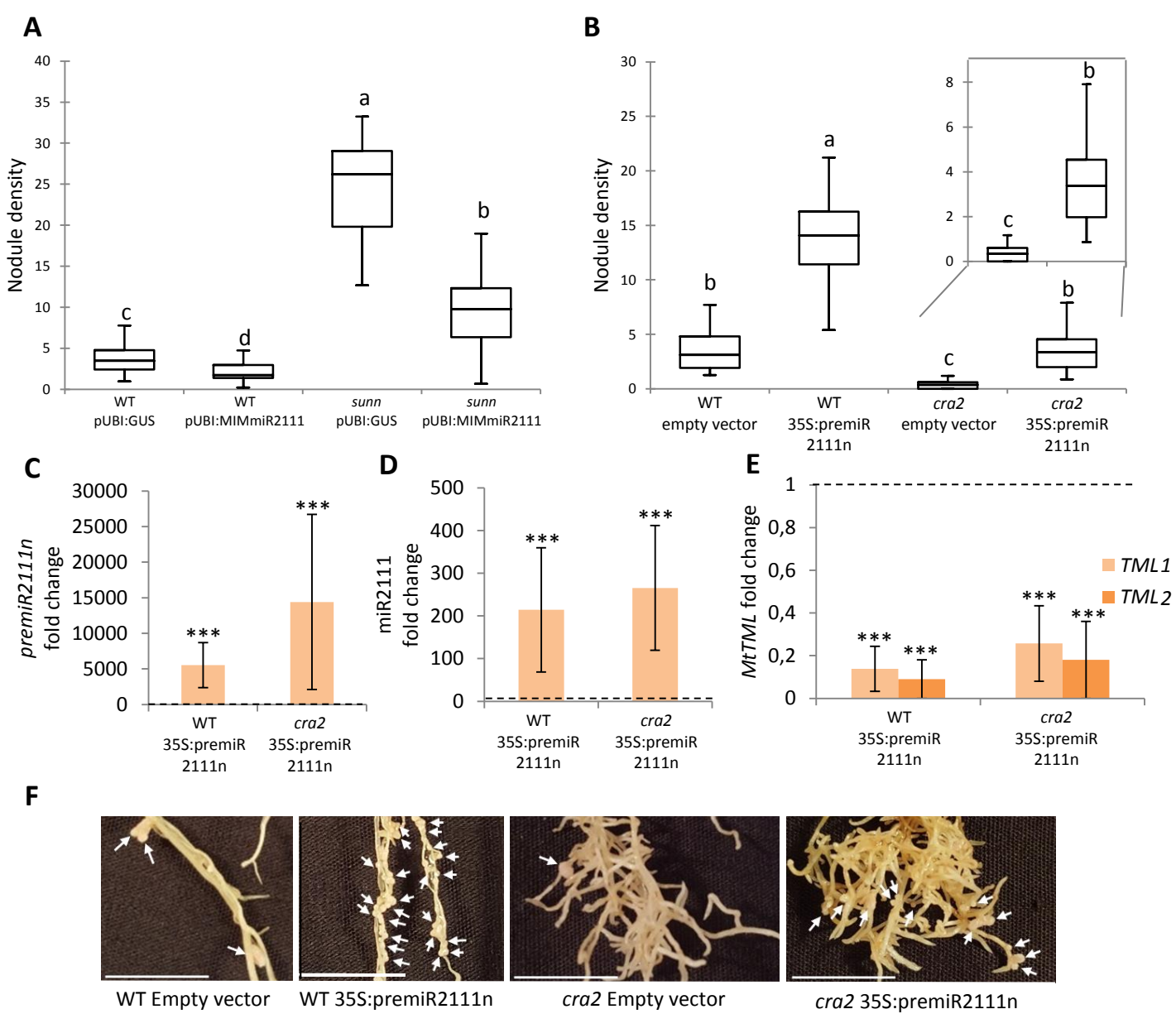
- 501 10. Tsikou, D., Yan, Z., Holt, D.B., Abel, N.B., Reid, D.E., Madsen, L.H., Bhasin, H.,  
502 Sexauer, M., Stougaard, J., and Markmann, K. (2018). Systemic control of legume  
503 susceptibility to rhizobial infection by a mobile microRNA. *Science*. *362*, 233–236.
- 504 11. Gautrat, P., Mortier, V., Laffont, C., De Keyser, A., Fromentin, J., Frugier, F., and  
505 Goormachtig, S. (2019). Unraveling new molecular players involved in the  
506 autoregulation of nodulation in *Medicago truncatula*. *J. Exp. Bot.* *70*, 1407–1417.
- 507 12. Oldroyd, G.E.D. (2013). Speak, friend, and enter: Signalling systems that promote  
508 beneficial symbiotic associations in plants. *Nat. Rev. Microbiol.* *11*, 252–263.
- 509 13. Tabata, R., Sumida, K., Yoshii, T., Ohyama, K., Shinohara, H., and Matsubayashi, Y.  
510 (2014). Perception of root-derived peptides by shoot LRR-RKs mediates systemic N-  
511 demand signaling. *Science*. *346*, 343–346.
- 512 14. Ohkubo, Y., Tanaka, M., Tabata, R., Ogawa-Ohnishi, M., and Matsubayashi, Y.  
513 (2017). Shoot-to-root mobile polypeptides involved in systemic regulation of nitrogen  
514 acquisition. *Nat. Plants* *3*, 1–6.
- 515 15. Wopereis, J., Pajuelo, E., Dazzo, F.B., Jiang, Q., Gresshoff, P.M., De Bruijn, F.J.,  
516 Stougaard, J., and Szczyglowski, K. (2000). Short root mutant of *Lotus japonicus* with  
517 a dramatically altered symbiotic phenotype. *Plant J.* *23*, 97–114.
- 518 16. Nishimura, R., Hayashit, M., Wu, G.J., Kouchi, H., Imaizumi-Anrakull, H., Murakami,  
519 Y., Kawasaki, S., Akao, S., Ohmori, M., Nagasawa, M., *et al.* (2002). HAR1 mediates  
520 systemic regulation of symbiotic organ development. *Nature* *420*, 426–429.
- 521 17. Pecrix, Y., Staton, S.E., Sallet, E., Lelandais-Brière, C., Moreau, S., Carrère, S., Blein,  
522 T., Jardinaud, M.F., Latrasse, D., Zouine, M., *et al.* (2018). Whole-genome landscape  
523 of *Medicago truncatula* symbiotic genes. *Nat. Plants* *4*, 1017–1025.
- 524 18. Formey, D., Sallet, E., Lelandais-Brière, C., Ben, C., Bustos-Sanmamed, P., Niebel, A.,  
525 Frugier, F., Combier, J.P., Debelle, F., Hartmann, C., *et al.* (2014). The small RNA  
526 diversity from *Medicago truncatula* roots under biotic interactions evidences the  
527 environmental plasticity of the miRNAome. *Genome Biol.* *15*, 1–21.
- 528 19. Magori, S., Oka-Kira, E., Shibata, S., Umehara, Y., Kouchi, H., Hase, Y., Tanaka, A.,  
529 Sato, S., Tabata, S., and Kawaguchi, M. (2009). Too Much Love, a root regulator

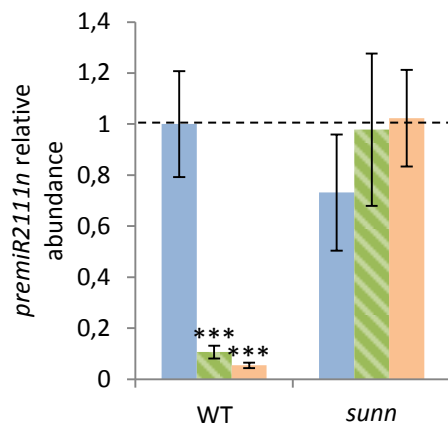
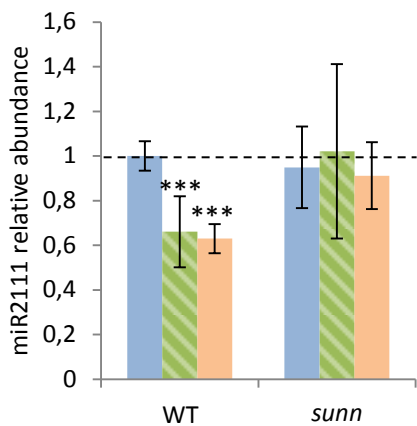
- 530 associated with the long-distance control of nodulation in *Lotus japonicus*. *Mol. Plant-*  
531 *Microbe Interact.* 22, 259–268.
- 532 20. Takahara, M., Magori, S., Soyano, T., Okamoto, S., Yoshida, C., Yano, K., Sato, S.,  
533 Tabata, S., Yamaguchi, K., Shigenobu, S., *et al.* (2013). TOO MUCH LOVE, a novel  
534 kelch repeat-containing F-box protein, functions in the long-distance regulation of the  
535 legume-rhizobium symbiosis. *Plant Cell Physiol.* 54, 433–447.
- 536 21. Devers, E.A., Branscheid, A., May, P., and Krajinski, F. (2011). Stars and symbiosis:  
537 Microna- and microna\*-mediated transcript cleavage involved in arbuscular  
538 mycorrhizal symbiosis. *Plant Physiol.* 156, 1990–2010.
- 539 22. Zhou, Z.S., Zeng, H.Q., Liu, Z.P., and Yang, Z.M. (2012). Genome-wide identification  
540 of *Medicago truncatula* microRNAs and their targets reveals their differential  
541 regulation by heavy metal. *Plant, Cell Environ.* 35, 86–99.
- 542 23. Terpolilli, J.J., O’Hara, G.W., Tiwari, R.P., Dilworth, M.J., and Howieson, J.G. (2008).  
543 The model legume *Medicago truncatula* A17 is poorly matched for N<sub>2</sub> fixation with the  
544 sequenced microsymbiont *Sinorhizobium meliloti* 1021. *New Phytol.* 179, 62–66.
- 545 24. Boisson-Dernier, A., Chabaud, M., Garcia, F., Bécard, G., Rosenberg, C., and Barker,  
546 D.G. (2001). *Agrobacterium rhizogenes*-transformed roots of *Medicago truncatula* for  
547 the study of nitrogen-fixing and endomycorrhizal symbiotic associations. *Mol. Plant-*  
548 *Microbe Interact.* 14, 695–700.
- 549 25. Frugier, F., Poirier, S., Satiat-Jeunemaître, B., Kondorosi, A., and Crespi, M. (2000). A  
550 Kruppel-like zinc finger protein is involved in nitrogen-fixing root nodule  
551 organogenesis. *Genes Dev.* 14, 475–482.
- 552 26. Karimi, M., Inzé, D., and Depicker, A. (2002). GATEWAY vectors for  
553 *Agrobacterium*-mediated plant. *Trends Plant Sci.* 7, 193–195.
- 554 27. Gouy, M., Guindon, S., and Gascuel, O. (2010). Sea view version 4: A multiplatform  
555 graphical user interface for sequence alignment and phylogenetic tree building. *Mol.*  
556 *Biol. Evol.* 27, 221–224.
- 557 28. Fahraeus, G. (1957). The infection of clover root hairs by nodule bacteria studied by a  
558 simple glass slide technique. *J. Gen. Microbiol.* 16, 374–381.

- 559 29. Blondon, F. (1964). Contribution à l'étude du développement des graminées  
560 fourragères ray-grass et dactyle. Thèse Doct. Etat, Fac. Sci., Paris, 131 p.
- 561 30. Weber, E., Engler, C., Gruetzner, R., Werner, S., and Marillonnet, S. (2011). A  
562 modular cloning system for standardized assembly of multigene constructs. PLoS One  
563 6, e16765.
- 564 31. Proust, H., Bazin, J., Sorin, C., Hartmann, C., Crespi, M., and Lelandais-Brière, C.  
565 (2018). Stable inactivation of microRNAs in *Medicago truncatula* roots. In Methods in  
566 Molecular Biology (Springer), pp. 123–132.
- 567 32. Lelandais-Brière, C., Naya, L., Sallet, E., Calenge, F., Frugier, F., Hartmann, C.,  
568 Gouzy, J., and Crespi, M. (2009). Genome-wide *Medicago truncatula* small RNA  
569 analysis revealed novel microRNAs and isoforms differentially regulated in roots and  
570 nodules. Plant Cell 21, 2780–2796.

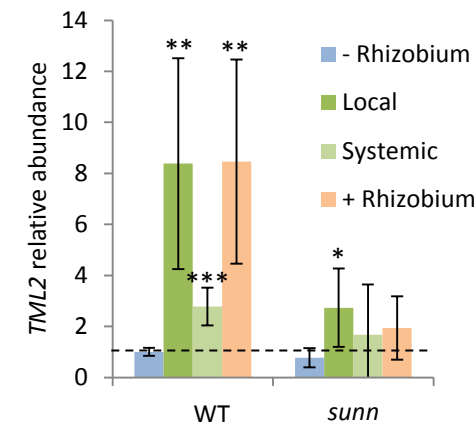
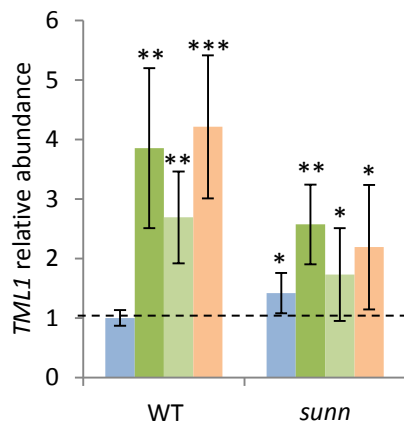
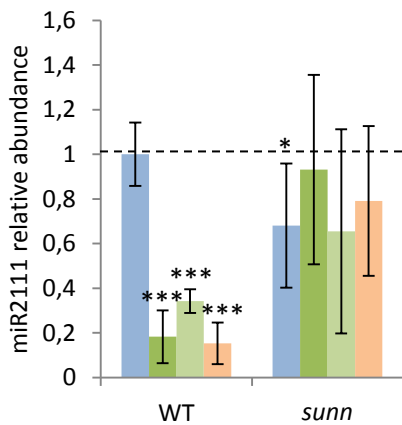
571

**A****B****C**

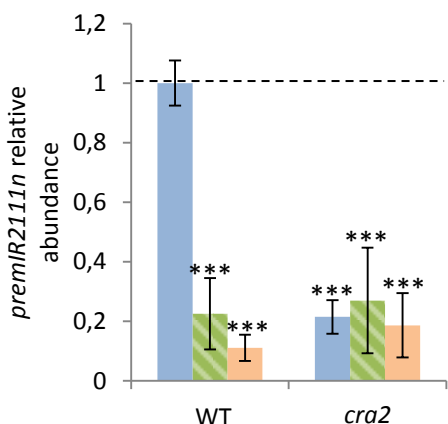
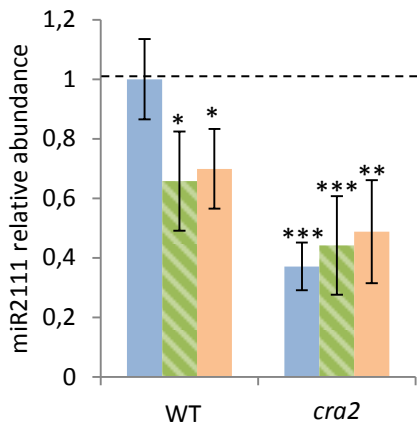


**A****Shoots**

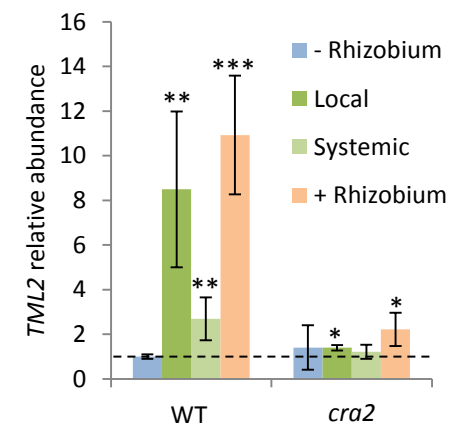
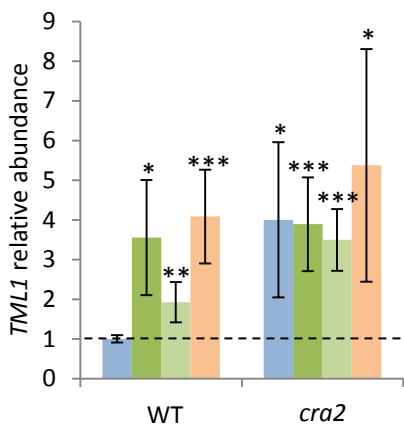
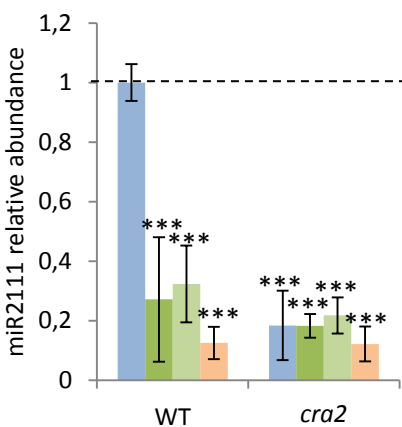
■ - Rhizobium  
 ■ Split  
 ■ + Rhizobium

**Roots**

■ - Rhizobium  
 ■ Local  
 ■ Systemic  
 ■ + Rhizobium

**B****Shoots**

■ - Rhizobium  
 ■ Split  
 ■ + Rhizobium

**Roots**

■ - Rhizobium  
 ■ Local  
 ■ Systemic  
 ■ + Rhizobium

